Hydrated DNA

DOI: 10.1002/anie.200905693

Ultrafast Vibrational Dynamics and Local Interactions of Hydrated DNA

*Łukasz Szyc, Ming Yang, Erik T. J. Nibbering, and Thomas Elsaesser**

Keywords:
energy dissipation · femtosecond vibrational spectroscopy · hydrated DNA · hydrogen bonds · water

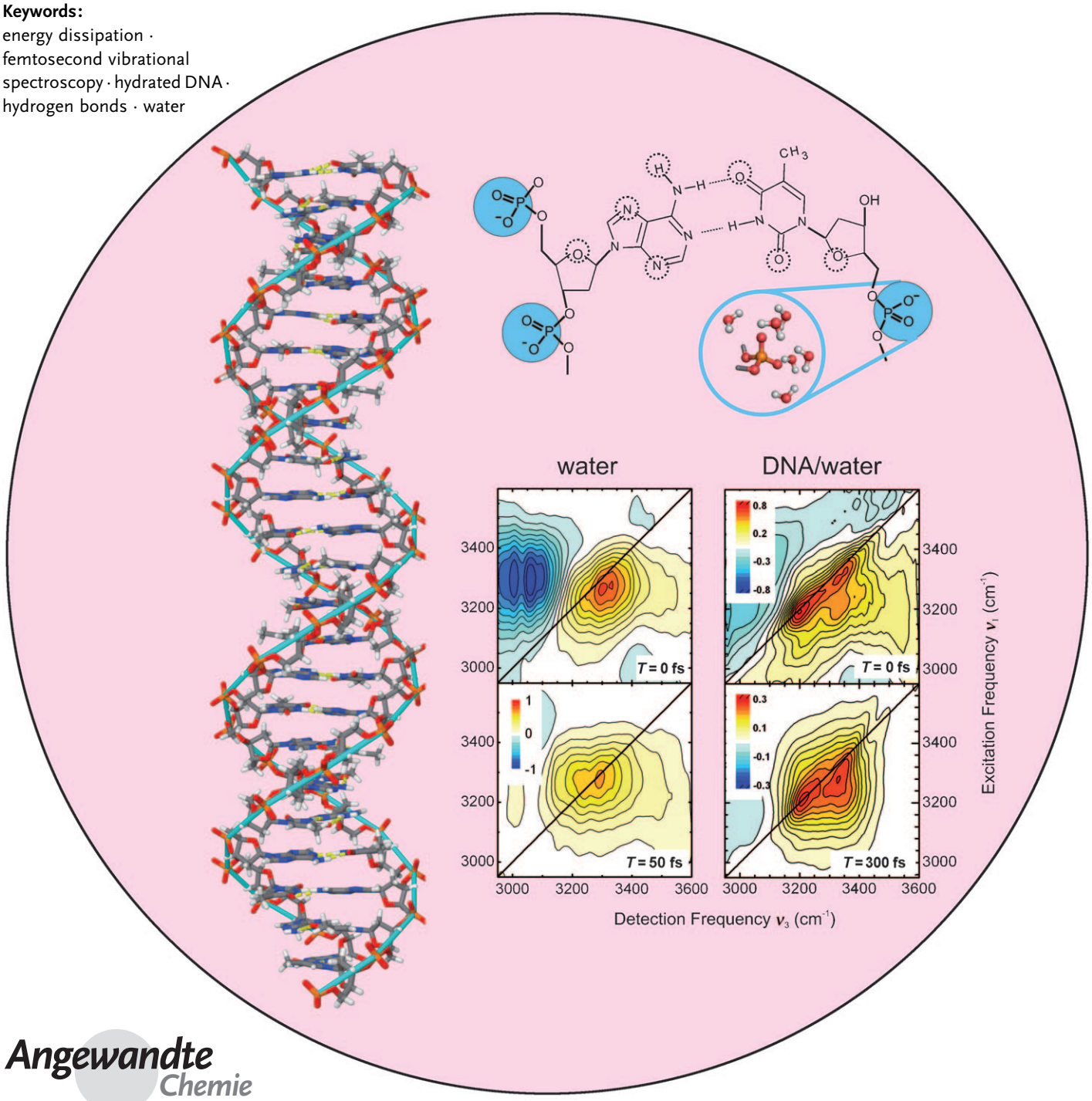

Angewandte International Edition Chemie

Biochemical processes occur mainly in aqueous environments, where interactions with water molecules play a key role for both the structure and function of biomolecules. Deoxyribonucleic acid (DNA), the basic carrier of genetic information, is characterized by an equilibrium double helix structure which is held together by intermolecular hydrogen bonds between base pairs and hydrated by an environment of water molecules with fluctuating hydrogen bonds. Basic vibrational motions of hydrated DNA and the fastest changes in the DNA–water interactions and hydration geometries occur in less than 1 ps. These processes can be accessed by mapping the vibrational dynamics of DNA and water in a time-resolved way by nonlinear ultrafast vibrational spectroscopy. Recent studies provide a detailed understanding of DNA vibrations and their dynamics, and give insight into nonequilibrium properties and structures of hydrated DNA.

From the Contents

1. Introduction

The interaction of DNA with surrounding water molecules is essential for stabilizing the macromolecular structure of the double helix and for electrically shielding charged or highly polar groups such as the phosphate groups in the DNA backbone and the counterions.[1–3] Changes in the hydration level result in conformational changes of the DNA helix, for example, a transition from the A form at a low water level into a fully hydrated B form.[4,5] The coupling of DNA and the aqueous environment allows for energy exchange and, thus, is expected to play a key role for non-equilibrium processes such as the dissipation of excess energy originating from the decay of electronic and/or vibrational excitations.

To date, the structure of hydrated DNA has mainly been studied under (quasi)stationary conditions by techniques such as X-ray diffraction, neutron scattering, and spectroscopic methods including vibrational spectroscopy.[2,6–10] These steady-state methods have enabled the highly precise characterization of the time-averaged structures of a large variety of DNA systems. DNA–water interactions were initially classified in terms of a first hydration shell consisting of water molecules directly interacting with particular functional groups of DNA and a second hydration shell with properties closer to bulk water.[2] This qualitative static picture has been refined by extensive nuclear magnetic resonance (NMR) studies, which have established interaction strengths and residence times of water molecules at particular binding sites.[4,11–13] Residence times at thermal equilibrium of approximately 10 ps up to the nanosecond range have been derived from NMR measurements at temperatures around 300 K. While such time scales are in agreement with theoretical molecular dynamics (MD) calculations, the simulations strongly suggest much faster intrinsic dynamics in the water shell around the DNA.[14,15]

At the molecular level, the interaction of DNA and water is characterized by a complex interplay of local hydrogen bonds and long-range Coulomb forces.[14–16] The structure of water and, thus, water–DNA interactions fluctuate on time scales between less than 50 fs and nanoseconds, with an average lifetime of the hydrogen bonds between water molecules of approximately 1 ps.[17–19] Elementary changes in molecular geometry such as fast rotations and/or reorientation and breaking of hydrogen bonds occur in the ultrafast time domain of up to a few picoseconds, a regime that NMR spectroscopy cannot address directly. In contrast, optical techniques with a femtosecond time resolution allow for ultrafast dynamics of hydrated DNA to be mapped in a time-resolved way and for different processes to be separated by their different time scales.

The dynamics of water at DNA interfaces have been studied by recording time-resolved fluorescence spectra of chromophores incorporated into the DNA structure.[20–22] The photoinduced change in the dipole moment of the chromophore induces a solvation process in which the energy of the excited emitting state is lowered by a reorientation of the surrounding water molecules. The picosecond time scale of such a change in the water structure has been derived from the time evolution of the concomitant red-shift of the emission, and has been analyzed by theoretical simulations.[22–24]

Vibrational spectroscopy addresses particular functional units within DNA and provides specific insight into local interactions. This selectivity allows the interaction of unsubstituted DNA with water to be studied in the electronic ground state.[7–10] In Figure 1, vibrational absorption spectra of bulk water (a) and DNA oligomers (b) at different hydration levels are shown (DNA structure shown in Figure 2 a,b). Although the line shapes of the different

[*] Ł. Szyc, M. Yang, Dr. E. T. J. Nibbering, Prof. Dr. T. Elsaesser
Max-Born-Institut für Nichtlineare Optik und Kurzzeitspektroskopie
Max-Born-Strasse 2A, 12489 Berlin (Germany)
E-mail: elsasser@mbi-berlin.de

bands reflect interactions in a time-integrated way, specific information on microscopic dynamics is very difficult to extract.

In recent years, nonlinear vibrational spectroscopy with femtosecond time resolution has developed into a major technique for investigating the ultrafast vibrational and related structural dynamics of aqueous systems, in particular of pure H_2O and isotopically diluted HOD in H_2O or D_2O.[25–43] The analysis of the nonlinear response allows the structural and relaxation dynamics to be separated by their intrinsic dynamics, and also allows intramolecular couplings, system–bath interactions, and relaxation times to be derived. Extensive theoretical work, to a large part based on MD simulations, has established a clear picture of the underlying microscopic processes. Ultrafast vibrational spectroscopy has also been applied to biomolecular model systems, including proteins, peptides, and light-harvesting complexes.[44] There are, however, a very limited number of studies on DNA.[45,46]

In this Review, we discuss new results on DNA–water interactions in the femto- to picosecond time domain. Different techniques of ultrafast infrared spectroscopy are applied to discern the NH stretching modes of adenine–thymine (A–T) base pairs in DNA oligomers from the OH stretching absorption of the surrounding water and to determine the dynamics and couplings of such vibrations. Measurements at different hydration levels allow for clear vibrational assignments. We then address vibrational dynamics of phosphate groups in the DNA backbone—major hydration sites that interact strongly with water. We demonstrate the important role of the phosphate hydration shells as a heat sink for the dissipation of excess energy from DNA and measure phosphate–water interactions in a time-resolved way.

The Review is organized as follows: Section 2 contains a summary of previous work on ultrafast vibrational and structural dynamics of bulk water as well as a discussion of existing knowledge on the vibrational properties of DNA under steady-state (equilibrium) conditions. Basic concepts of femtosecond vibrational spectroscopy and the preparation of thin-film DNA samples are discussed in Section 3. New results on vibrational dynamics and couplings of hydrated DNA are presented in Section 4, followed by results on ultrafast hydration dynamics (Section 5). A summary and a brief outlook are given in Section 6.

Left to right: M. Yang, Ł. Szyc, E. Nibbering, T. Elsaesser

Ming Yang was born in 1979 in Nanjing (China). He completed his bachelor degree at the National University of Defense Technology (Changsha) in 2000. In 2007, he finished his Masters at the Shanghai Institute of Optics and Fine Mechanics, Chinese Academy of Science, where he studied the interaction between matter and ultrafast and ultraintensive laser pulses (supervisor Prof. Jiansheng Liu). Since 2007, he has been a PhD student at the Max Born Institut, where he is investigating the ultrafast dynamics of hydrogen bonds in DNA model systems.

Łukasz Szyc was born in Sieradz (Poland) in 1982. He received his Masters degree in Chemistry from Wrocław University in 2006, where he studied secondary structure transitions in polypeptides. In 2007, he started PhD research at the Max Born Institut, where he is investigating the ultrafast dynamics of biologically relevant hydrogen-bonded systems, in particular hydrated DNA films.

Erik T. J. Nibbering (born in 1965) studied chemistry at the Vrije Universiteit (Amsterdam, the Netherlands), and received his diploma in physical chemistry in 1988. For his PhD research he investigated femtosecond optical dephasing and solvation dynamics in liquids with Prof. D. A. Wiersma at the Rijksuniversiteit Groningen (1988–1993). After two years research at the Laboratoire d'Optique Appliqueé—E.N.S.T.A.—École Polytechnique (Palaiseau, France) with Prof. A. Mysyrowicz, he joined the Max Born Institut in 1995, and became project leader in 1997 and department head in 2003. He completed his Habilitation in experimental physics in 2007 at the FU Berlin. His research interests include the generation of ultrafast light pulses and ultrafast spectroscopy resolving structural dynamics of condensed matter.

Thomas Elsaesser (born in 1957) studied physics at the University of Heidelberg and the Technical University of Munich. In 1986 he completed his PhD with Prof. W. Kaiser at the TU Munich on picosecond infrared spectroscopy. After working as a research associate at the TU Munich and postdoctoral research at AT&T Bell Laboratories, Holmdel, USA, he finished his Habilitation at the TU Munich in 1991. Since 1993, he has been director of the Max Born Institut and Professor for Experimental Physics at the Humboldt University, Berlin. He has contributed to a broad range of research in ultrafast science, particularly processes in condensed matter. His major interests are transient structures of as well as basic microscopic interactions in (bio)molecular systems and solids.

2. Vibrational Properties of Bulk Water and Hydrated DNA

2.1. Ultrafast Vibrational and Structural Dynamics of Liquid H_2O

In the liquid phase, water molecules form an extended disordered network of intermolecular hydrogen bonds.[17,18] A single water molecule can donate two hydrogen bonds through its hydrogen atoms and accept two hydrogen bonds to the oxygen atom (Figure 1 a). This molecular network undergoes structural fluctuations in the ultrashort time range between approximately 10 fs, the period of the OH stretching vibration, and several picoseconds. As a consequence of the highly polar character of the water molecule, structural fluctuations result in fluctuating long-range Coulomb interactions. The vibrational absorption spectrum in the frequency range between 600 and 4000 cm^{-1} (Figure 1 a) is dominated by the fundamental $v=0$ to $v=1$ ($v=0\rightarrow1$) transitions of the intramolecular OH stretching and bending modes and by librations, that is, hindered rotational motions of water molecules in the network. The strong OH stretching band

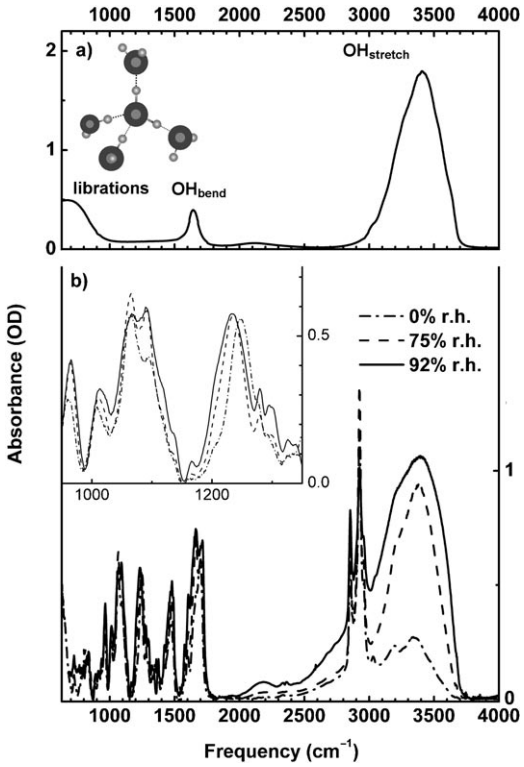

Figure 1. a) Infrared absorption spectrum of liquid water (H_2O) consisting of the OH stretching band, the OH bending absorption, and the L2 librational band ($T = 300$ K, sample thickness 3 μm). The absorption between 1000 and 1600 cm^{-1} is due to high-frequency librations, and the weak band at 2100 cm^{-1} to a libration/OH bend combination tone. Inset: tetrahedral geometry of hydrogen-bonded water molecules. b) Infrared absorption spectrum of DNA oligomers containing 23 alternating adenine–thymine base pairs (structure shown in Figure 2a,b). The thin-film sample on a Si_3N_4 substrate is held at hydration levels of 0%, 75%, and 92% relative humidity (r.h.). The band between 3000 and 3700 cm^{-1} is due to NH stretching vibrations of base pairs and the OH stretching mode of water. Inset: Infrared absorption in the range of the symmetric (1070 cm^{-1}) and asymmetric (1250 cm^{-1}) $(PO_2)^-$ stretching vibrations of the phosphate groups in the DNA backbone. Both bands show characteristic changes upon hydration.

reaches a maximum at 3400 cm^{-1}, and the OH bending absorption at 1650 cm^{-1}. The librational absorption covers a broad range from 400 to 1600 cm^{-1}, with the intense L2 band around 670 cm^{-1} and the weak OH bend/libration combination tone at 2100 cm^{-1}. The absorption arising from translational motions occurs below 400 cm^{-1}, as does the O···O hydrogen bond mode (at 170 cm^{-1}).

The ultrafast dynamics of water have mainly been studied by pump-probe and photon echo experiments with a femtosecond time resolution. Such techniques are described in detail in Section 3. The experiments have shown that fluctuating Coulomb forces lead to strong spectral diffusion, that is, stochastic frequency jumps of OH stretching oscillators.[30–41] The $v = 0 \rightarrow 1$ transition frequency of a particular OH stretching oscillator explores a major part of the frequency range covered by the OH stretching absorption band. Two-dimensional spectra of the OH stretching mode of H_2O have shown that the fastest components of the fluctuating force in the sub-50 fs range are related to high-frequency librational motions of water molecules.[40,41] In addition, there are slower (sub)picosecond contributions that reflect water rotations and the breaking and reformation of hydrogen bonds.[34] Resonant energy transfer of OH stretching excitations between different water molecules occurs on a 100 fs time scale,[40,41,43] and also contributes to spectral diffusion. The observed behavior is in agreement with extensive theoretical work based on MD simulations of water dynamics.[33–39] In particular, the projection of the fluctuating electric field on the O–H bonds of the water molecules has been identified as a key quantity that generates the observed frequency fluctuations.

The lifetime of the $v = 1$ state of the OH stretching and OH bending oscillator is 200 fs and 170 fs, respectively.[40,41,47–50] The $v = 1$ OH stretching and the $v = 2$ OH bending states are in (Fermi) resonance. Femtosecond pump-probe experiments have demonstrated the cascaded decay of the OH stretching vibration via the $v = 2$ and $v = 1$ states of the OH bending mode and the concomitant disposal of excess energy into intermolecular modes of the hydrogen-bond network.[50] Very recent theoretical studies have shown that the $v = 1$ OH bending excitation predominantly decays into a hindered rotation of the bend-excited molecule, with centrifugal coupling representing the main interaction mechanism between the two modes.[51,52] High-frequency librations in the range between 1000 and 1600 cm^{-1} display a so-far unresolved lifetime of less than 100 fs. Their decay leads to a local weakening of hydrogen bonds around the excited molecules, followed by a slower delocalization of excess energy in the network.[50] The latter process is characterized by time constants of the order of 1 ps, and involves the breaking of hydrogen bonds. Within a few picoseconds, a macroscopically heated ground state of the network is established, which is characterized by an elevated temperature and—in time average—an enhanced fraction of broken hydrogen bonds. The breaking of hydrogen bonds involves a large-angle rotational motion of a water molecule from its original to its new binding partner, and is induced by fluctuations in the coordination number of the water molecule.[42] The occurrence of such fluctuations increases with temperature.

2.2. Vibrational Properties and Hydration Shells of DNA

The linear infrared and Raman spectra of DNA and their change upon hydration have been the subject of extensive experimental studies and theoretical calculations.[7–10,53–58] Vibrational bands of DNA cover a very broad frequency range—from the high-frequency stretching vibrations of NH or CH groups between 2800 and 3700 cm^{-1} down to sub-1 cm^{-1} excitations that involve highly delocalized motions of the DNA backbone. In general, the infrared and Raman spectra are highly congested with many overlapping bands, in particular in the fingerprint range between 1000 and 2000 cm^{-1}. Above 3000 cm^{-1}, the assignment of different bands to NH and NH_2 stretching excitations of base pairs has remained controversial, in particular when comparing theoretical calculations and experiments.[56–58]

In Figure 1b we present the steady-state infrared spectra of the DNA film samples studied in our femtosecond experiments for different levels of relative humidity (r.h.). The samples contain DNA oligomers with 23 alternating adenine–thymine (A–T) base pairs (Figure 2a,b) and cetyl-

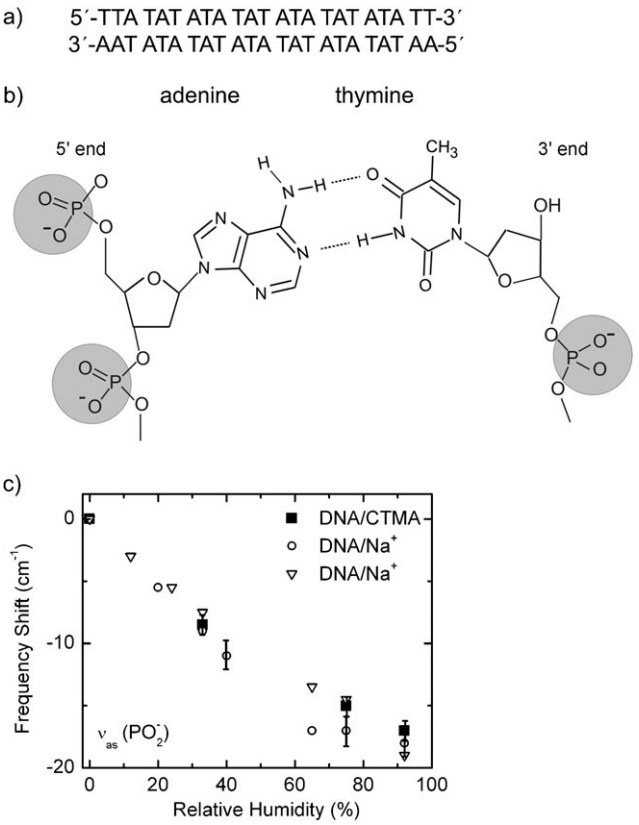

Figure 2. a) Sequence of alternating adenine–thymine (A–T) base pairs in the artificial double-stranded DNA oligomers. b) Molecular structure of the A–T base pairs together with the sugar units and the ionic phosphate groups of the DNA backbone. The shaded areas around the phosphate groups symbolize their hydration shells. c) Frequency shift of the asymmetric $\nu_{as}(PO_2)^-$ stretching vibration as a function of the relative humidity (r.h.) in the sample. Data for the DNA/CTMA complexes (squares) studied here are compared to results for DNA with Na^+ counterions (Refs. [9, 60]).

trimethylammonium counterions. In the frequency range above 3000 cm^{-1}, the sample at 0% r.h. (2 water molecules per base pair) shows a broad absorption with some substructure.[59] Increasing the water content to 75% r.h. (12 water molecules per base pair) and 92% r.h. (>20 water molecules per base pair) enhances and reshapes this absorption substantially, mainly as a result of the enhanced OH stretching absorption at the higher water concentration. It should be noted, however, that the absorption strength does not simply scale with the water concentration, that is, the increase in the maximum absorbance (at 3400 cm^{-1}) from 0 to 92% r.h. is much less than expected from the ratio of the water concentrations. This fact demonstrates that the band observed at 0% r.h. cannot be entirely due to water but contains contributions from DNA vibrations.

The inset in Figure 1b shows the changes in the symmetric and asymmetric $(PO_2)^-$ stretching bands of the phosphate groups in the DNA backbone upon increasing the hydration level. The asymmetric stretching band $\nu_{as}(PO_2)^-$ exhibits a continuous red-shift with increasing water concentration, which is shown in more detail in Figure 2c (squares). This behavior is in line with extensive earlier work on DNA with sodium counterions. Slightly different frequency positions of the $\nu_{as}(PO_2)^-$ band arising from the different polarity of the counterion were found, but identical shifts were observed upon changes in the hydration level (open symbols).[9,60] We will use this mode as a sensitive probe of hydration dynamics in the time-resolved experiments.

On the basis of such and related results from infrared spectroscopy, Falk et al. have proposed a (static) hydration scheme of DNA, in which the sodium counterion of DNA and the phosphate groups represent the main hydration sites. In contrast, hydrogen bonds to the sugar groups in the backbone and to functional groups of the base pairs are substantially weaker.[8,9] The few water molecules at 0% r.h. are thus expected to be located near the phosphate units. Besides vibrational spectroscopy, DNA hydration has been studied by other techniques such as X-ray diffraction, neutron scattering, and NMR, all complemented by theoretical studies, in particular MD simulations. The role of phosphate groups as the main hydration sites and hydration geometries in the major and minor grooves of the DNA double helix have been elucidated in detail. X-ray and neutron scattering suggest that six water molecules interact with the two free oxygen atoms in fully hydrated DNA.[6] Each phosphate group is surrounded by its own hydration shell, which is spatially separated and, thus, weakly interacting with the water shells of neighboring phosphate groups. In an aqueous environment, the first "layer" of water molecules directly interacting with the DNA (for example, through hydrogen bonds) is complemented by water molecules at larger distances that interact through long-range Coulomb interactions.[2,6] Differentiation between the different water species has remained difficult beyond this qualitative concept of a "second hydration shell". Moreover, all results discussed so far characterize the steady-state behavior of DNA close to thermal equilibrium.

3. Femtosecond Nonlinear Vibrational Spectroscopy and DNA samples

3.1. Femtosecond Nonlinear Vibrational Spectroscopy

Femtosecond infrared spectroscopy is based on the resonant interaction of femtosecond light pulses with vibrational dipole transitions.[25,26,61,62] In the following, we briefly describe the pump-probe technique and two-dimensional vibrational spectroscopy, both mapping the third-order nonlinear response of an ensemble of molecular oscillators. Femtosecond resonant excitation of a transition between two quantum states of an oscillator (Figure 3a) generates both a coherent polarization, that is, a dipole-mediated superposition of the wave functions of the two states, and a population change by promoting molecules from the lower to the upper

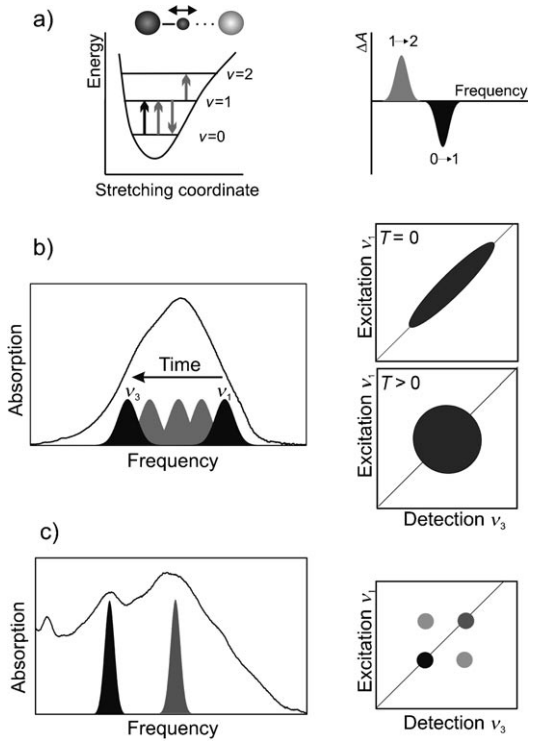

Figure 3. a) Left: Schematic representation of a linear hydrogen bond with an X–H donor group (dark spheres) and a Y acceptor atom (light sphere) as well as the potential-energy diagram of an anharmonic oscillator with quantum states $v=0$, 1, and 2. In a femtosecond pump-probe experiment, the $v=0\rightarrow1$ transition is excited by the pump pulse (black arrow) and both the $v=0\rightarrow1$ and $v=1\rightarrow2$ transitions are probed (gray arrows). Right: Schematic representation of the changes in the measured absorption with a decrease of $v=0\rightarrow1$ absorption and a red-shifted increase of $v=1\rightarrow2$ absorption. b) Left: OH stretching absorption band of H_2O with the principle of spectral diffusion. Right: Schematic representation of two-dimensional (2D) spectra for different population times T. c) Left: NH/OH stretching absorption of the DNA oligomers of Figure 2 for 0% r.h. and their spectral components. Right: Schematic 2D spectrum with diagonal and off-diagonal peaks.

state. In the pump-probe approach, this excitation is probed by a second pulse that monitors changes of vibrational absorption as a function of pump-probe delay. In Figure 3a, the pump pulse (black arrow, left panel) excites the $v=0\rightarrow1$ transition of a stretching oscillator and the system is probed through changes in the $v=0\rightarrow1$ and $v=1\rightarrow2$ absorption (gray arrows). For a sequential interaction, that is, the probe interacts after the pump, the reduced population of the $v=0$ state and the excess population of the $v=1$ state lead to a change in the absorption $\Delta A<0$ on the $v=0\rightarrow1$ transition as a result of bleaching and stimulated emission (black profile in the right panel of Figure 2a). Concomitantly, the $v=1$ excess population gives rise to an enhanced absorption $\Delta A>0$ on the $v=1\rightarrow2$ transition (gray profile). The latter component is shifted to lower frequency because of the anharmonicity of the oscillator. Measuring ΔA as a function of pump-probe delay gives insight into population kinetics and the related redistribution of energy.

In two-dimensional (2D) infrared spectroscopy, a sequence of three infrared pulses of femtosecond duration interacts with the molecular sample and induces a coherent vibrational response which is read-out via the so-called photon-echo signal.[63–66] There are two independent time intervals between pulse 1 and 2—the coherence time τ—and between pulse 2 and 3—the waiting or population time T. The photon echo signal can be detected in a time-integrated way (homodyne detection) or in a phase-resolved way by mixing it with the electric field of a reference pulse (pulse 4), the local oscillator (heterodyne detection). From the heterodyne signal, one derives 2D spectra, in which the Fourier transform of the third-order polarization of the sample is plotted as a function of two frequencies—the excitation frequency ν_1 and the detection frequency ν_3. The real part of this quantity gives the absorptive response, the imaginary part the dispersive response of the sample. (Further details of this method can be found in Refs. [64,66].)

Figure 3b shows the case where spectral diffusion predominates. In a disordered hydrogen-bond network, such as bulk water, the $\nu_{OH}=0\rightarrow1$ transition frequency of the OH stretching mode depends on the local environment, resulting in a (inhomogeneous) frequency distribution within the OH stretching absorption band (left panel). As the structure of the network and, thus, both the local environments and the long-range Coulomb interactions of the molecules fluctuate, the frequency position of a particular oscillator changes with time, undergoing statistical frequency shifts within the spectral envelope—the so-called spectral diffusion. Time-resolved 2D absorption spectra (right panel of Figure 3b) make spectral diffusion directly visible. The 2D spectra for $T=0$, that is, when the frequency distribution of the excited oscillators generated by the first two pulses is read-out instantly by the third pulse, display an elongated shape along the diagonal $\nu_1=\nu_3$. This means that for each frequency ν_1 there is a signal at the corresponding detection frequency ν_3. During a finite time interval T between the second and the third "read-out" pulse, the molecular system undergoes spectral diffusion, thereby destroying the correlation of the excitation and detection frequencies. As a result, the 2D spectrum measured for $T>0$ shows an essentially round shape which reflects the randomization of transition frequencies and the underlying molecular geometries.

In the opposite case of negligible spectral diffusion, 2D spectra allow couplings between different vibrational transitions to be deciphered in a quantitative way. This is illustrated in Figure 3c by using the NH/OH stretching absorption of DNA oligomers as an example. The linear absorption band consists of a number of lines, which result in the highly complex spectral envelope. Different types of peaks occur in the nonlinear 2D spectra: Excitation of a particular line (black or gray profile in the linear spectrum) results in a signal at the same frequency on the diagonal of the 2D spectrum (black and gray symbols in the right panel), and—in addition—in an off-diagonal peak at the frequency position of the other coupled transition (light gray symbols). The strength of the off-diagonal peaks is proportional to the strength of the couplings.

The results presented in Sections 4 and 5 originate from two-color pump-probe experiments in a wide frequency range of 1000 to 4000 cm^{-1} and heterodyne-detected photon echo studies between 3000 and 3700 cm^{-1}. Pump and probe pulses of 150 cm^{-1} spectral width (FWHM) which can be tuned independently in the range of 800 to 3700 cm^{-1} were generated in two parametric frequency converters.[67] The energy of the pump pulses at the sample was 1.5 μJ, resulting in an excitation of less than 5% of the oscillators in the sample. The temporal width of the cross-correlation of the pump and probe pulses was 150 fs (FWHM). The change of absorbance of the DNA films $\Delta A = -\log(T/T_0)$ (T,T_0: sample transmission with and without excitation) was measured as a function of the pump-probe delay with parallel (ΔA_{par}) and perpendicular (ΔA_{pp}) linear polarization of the pump and probe pulses. From such data, the time-dependent pump-probe anisotropy $r(t) = (\Delta A_{par} - \Delta A_{pp})/(\Delta A_{par} + 2\Delta A_{pp})$ was derived. After interaction with the sample, the probe pulses were spectrally dispersed and detected with a HgCdTe detector array with 16 elements (resolution 2 cm^{-1} around 1200 cm^{-1} and 8 cm^{-1} between 3000 and 3700 cm^{-1}).

The photon echo experiments were performed with a setup that used diffractive optics for generating phase-locked pulse pairs with propagation directions ($\mathbf{k_1}$,$\mathbf{k_2}$) and ($\mathbf{k_3}$,$\mathbf{k_{LO}}$) in a so-called box-car geometry of beams that interact with the sample.[40,41] 2D spectra were derived from the heterodyne detected signal in the $\mathbf{k_1}$-$\mathbf{k_2}$+$\mathbf{k_3}$ direction by the method detailed in Refs. [40,41]. In general, elastic scattering of infrared light from the DNA films and the substrate generates a background signal in the detection of the photon echo signal. This background signal is sufficiently small in the case of DNA films on CaF_2 substrates that photon echo measurements can be performed both in homo- and heterodyne detection.

3.2. Preparation of DNA Thin-Film Samples

In the femtosecond experiments, DNA oligomer duplexes containing 23 alternating adenine–thymine (A–T) base pairs were studied. The duplexes consist of a 5′-T$(TA)_{10}$-TT-3′ strand and its complement (Figure 2a,b). To generate DNA films of high optical quality, the sodium counterions are replaced by the surfactant cetyltrimethylammonium (CTMA), which forms complexes with DNA. DNA thin-film samples of 5–30 μm thickness were prepared by a procedure described in detail in Refs. [68–71]. The complexes were cast on 0.5 μm thick Si_3N_4 or 1 mm thick CaF_2 substrates. From the size of the DNA/surfactant complexes, a DNA concentration of 1.5×10^{-2} M can be estimated. The DNA samples were integrated into a home-built humidity cell. This cell was connected to a reservoir containing various agents to control the relative humidity (r.h.) in the cell and the DNA film. The water concentration in the film was 0.57 M, 3.5 M, and 5.7 M for 0%, 75%, and 92% r.h., respectively. The hydration level of the DNA films was verified by steady-state infrared measurements of the $\nu_{as}(PO_2)^-$ absorption at the different humidity levels (Figure 2c) and by gravimetric studies.

X-ray diffraction studies have shown that DNA complexed with surfactant counterions undergoes water-content-driven changes in its helix conformation very similar to DNA with standard Na^+ counterions.[68–70] DNA oligomers with alternating A–T pairs exist in the D conformation[2] between 40 and 70% r.h. and in the B conformation[2] at higher humidity levels. X-ray diffraction studies on thin films also show a well-defined helix structure at 0% r.h.

4. Ultrafast Vibrational Dynamics and Couplings of Hydrated DNA

4.1. NH and NH_2 Stretching Vibrations of DNA Base Pairs

The NH and NH_2 stretching bands of thymine and adenine were assigned and discerned from the OH stretching absorption of water in spectrally and temporally resolved pump-probe measurements at different hydration levels.[59,71] Nonlinear absorption spectra for different time delays after excitation by pulses centered at $E_{ex} = 3250$ cm^{-1} are presented in Figure 4. At 0% r.h. (Figure 4a), a spectrally broad enhanced absorption is observed below 3100 cm^{-1} as a result of the $v = 1 \rightarrow 2$ transitions of the excited oscillators. The two pronounced negative peaks with maxima at 3200 and 3350 cm^{-1} originate from bleaching and stimulated emission on the $v = 0 \rightarrow 1$ transitions. The amplitudes of such signals decrease on a 1 ps time scale without changing the spectral positions, pointing to a minor role of spectral diffusion. The

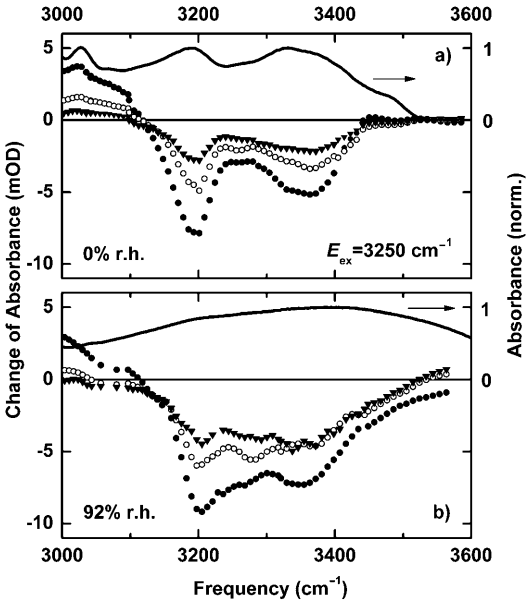

Figure 4. a) Transient pump-probe spectra (symbols) of DNA oligomers at 0% r.h after excitation by femtosecond pulses centered at $E_{ex} = 3250$ cm^{-1}. The change of absorbance $\Delta A = -\log(T/T_0)$ (T, T_0: sample transmission with and without excitation, parallel polarization of pump and probe) in mOD is plotted as a function of the probe frequencies for pump-probe delays of 100 fs (solid circles), 500 fs (open circles), and 1 ps (triangles). The solid line gives the linear absorption spectrum. b) Corresponding data for DNA oligomers at 92% r.h.

time evolution of enhanced absorption ($v=1\rightarrow2$ transition) and bleaching ($v=0\rightarrow1$ transition) shown in Figure 5a,b for two fixed spectral positions (solid circles) displays an initial relaxation with the lifetime of the excited $v=1$ states of approximately 500 fs. Sub-picosecond Raman experiments

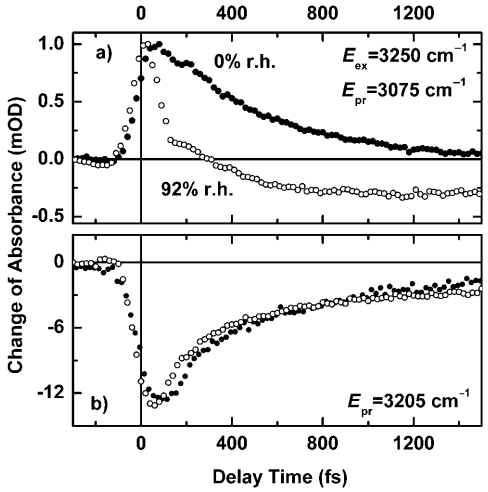

Figure 5. a) Change of absorbance ΔA at a probe photon energy of $E_{pr}=3075$ cm^{-1} after excitation of the DNA oligomers at $E_{ex}=3250$ cm^{-1} plotted as a function of pump-probe delay. Data are for 0% r.h. (solid circles) and 92% r.h. (open circles, parallel polarizations of pump and probe). b) Corresponding data for a probe photon energy of $E_{pr}=3205$ cm^{-1} (ΔA values scaled for comparison of 0% and 92% r.h.).

have shown that the NH excitations decay predominantly into fingerprint modes in the frequency range of the NH bending vibrations.[72] After the 500 fs recovery, the absorption decrease in Figure 5b shows a much slower long-lived signal that is related to the dissipation of excess energy, which will be discussed in Section 5.

The transient spectra of the fully hydrated sample (92% r.h.) are shown in Figure 4b. The two prominent negative peaks at 3200 and 3350 cm^{-1} are now complemented by a broad OH stretching absorption of the additional water molecules which is most pronounced between the two bands and above 3400 cm^{-1}. As shown in Figure 5a,b (open circles), the time evolution of the absorption changes is somewhat altered at 92% r.h. In particular, there is a fast decay of the enhanced absorption at 3075 cm^{-1} (Figure 5a), followed by a slower component which levels off at a slightly negative value.

A detailed analysis of the two transient bands at 3200 and 3350 cm^{-1}, including measurements of transient pump-probe anisotropies and taking into account vibrational assignments from gas-phase studies of isolated base pairs, has been presented in Refs. [59,71]. The band at 3200 cm^{-1} represents a superposition of the NH stretching band of thymine and the symmetric NH_2 stretching band of adenine, while the band at 3350 cm^{-1} is due to the asymmetric NH_2 stretching mode of adenine. The NH stretching mode of thymine and the symmetric NH_2 stretching mode of adenine display a vibrational coupling of the order of 15 cm^{-1}, which was derived from the decay of the pump-probe anisotropy.[71] Compared to this coupling, their coupling to the asymmetric NH_2 stretching mode is less pronounced. Coupling between oscillators located on different base pairs is expected to be even weaker and is not observed here.

The femtosecond measurements presented so far allow the different NH stretching bands of the base pairs and the mutual couplings of the different oscillators to be identified. The results for different hydration levels clearly show that the NH stretching bands make a prominent contribution to the steady-state absorption in the range of 3000 to 3700 cm^{-1}.

4.2. OH Stretching Dynamics of Water Interacting with DNA

The OH stretching mode of water is a sensitive probe of the structure and dynamics of both local hydrogen bonding and long-range Coulomb interactions. The OH stretching absorption occurs in the same spectral range as the NH stretching bands of the DNA base pairs. Transient pump-probe spectra of the DNA samples measured after excitation around $E_{ex}=3550$ cm^{-1} are presented in Figure 6. At 0% r.h. (Figure 6a), the two water molecules per base pair give rise to

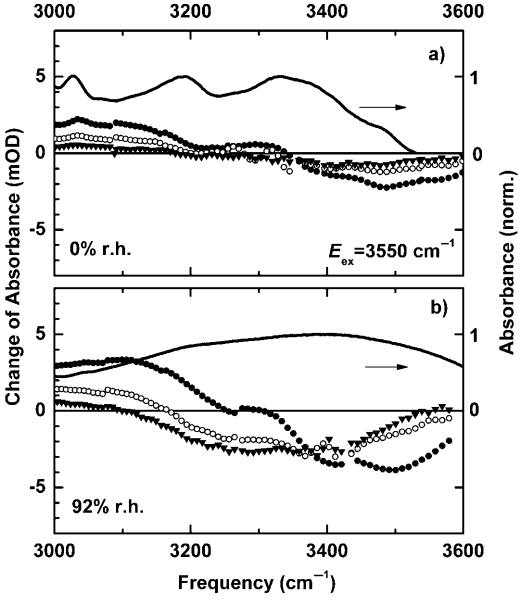

Figure 6. a) Transient pump-probe spectra of DNA oligomers at 0% r.h after excitation by femtosecond pulses centered at $E_{ex}=3550$ cm^{-1}. The change of absorbance ΔA in mOD is plotted as a function of probe frequencies for pump-probe delays of 100 fs (solid circles), 500 fs (open circles), and 1 ps (triangles, parallel polarizations of pump and probe). The solid line gives the linear absorption spectrum. b) Corresponding data for DNA oligomers at 92% r.h.

a weak OH stretching band with a maximum at 3480 cm^{-1}. This band displays negligible spectral diffusion and decays on a time scale of a few picoseconds. The $v=1$ lifetime of the OH stretching mode of about 500 fs (not shown) is substantially longer than in bulk water (200 fs, see Section 2.1). The pump-probe anisotropy has a time-independent value of 0.4 rather than the 100 fs decay observed in neat H_2O. Such results point to a hydration pattern in which individual water molecules are attached to the phosphate groups—the strongest hydrogen-

bond acceptor in the DNA samples. The spectral position of the OH stretching band and the longer $v=1$ lifetime are similar to the behavior of water in small reverse micelles, where water molecules interact directly with the highly polar or ionic head groups of the micelle.[73,74] In the water–DNA case, the strong local interaction leads to a binding geometry in which the water molecules are sterically fixed, and rotational motions that would result in changes of anisotropy are essentially suppressed.

At 92% r.h., where there are more than 20 water molecules per base pair, a much more heterogeneous structure of water is expected. In addition to water molecules interacting directly with DNA through local hydrogen bonds, an outer hydration shell should exist where interactions between water molecules predominate, similar to neat H_2O. The pump-probe data in Figures 4 and 6 indeed give evidence for different water species. The transient OH stretching band (Figures 4b and 6b) covers a much wider spectral range from approximately 3200 to 3600 cm^{-1}. After excitation at $E_{ex}=$ 3550 cm^{-1}, the transient OH stretching band displays pronounced spectral diffusion, which results in a shift towards lower frequencies (Figure 6b).

Time-resolved transients for 92% r.h. are shown in Figure 7a. The decrease of OH stretching absorption after excitation at $E_{ex}=3500$ cm^{-1} displays an initial recovery with a time constant of 200 fs, which matches the fast decay of the $v=1\rightarrow2$ absorption in Figure 5a, and is close to the lifetime of the $v=1$ state in bulk water. This kinetic component is followed by a slower contribution with a time constant of about 500 fs and—eventually—by a long-lived residual signal that remains constant for hundreds of picoseconds. We compare this transient with data taken with excitation pulses centered at $E_{ex}=3250$ cm^{-1} (diamonds in Figure 7). Here again, the 200 fs component of bleaching recovery is found which now, however, is followed by the 500 fs build-up of a long-lived transient absorption. This behavior is very similar to bulk water, as shown by comparison with a bulk water transient measured with the same pump and probe frequencies (solid line, Ref. [47]). The enhanced absorption reflects the formation of a vibrationally hot ground state in the water shell. The excess energy originating from the decay of the OH stretching excitation is eventually transferred to intermolecular low-frequency modes and delocalized in the hydrogen-bond network. This results in a rise of vibrational temperature of 3–5 K under our experimental conditions. In the heated water network, the fraction of broken hydrogen bonds is larger, that is, on average the fraction of OH groups not being part of a hydrogen bond is increased. The stretching absorption of such OH groups occurs at the high-frequency edge of the OH stretching band, thereby giving rise to the enhanced absorption.

Two-dimensional (2D) vibrational spectra give more specific insight into the time scales and mechanisms of spectral diffusion. As illustrated schematically in Figure 3b, a correlation of excitation and detection frequencies is found in an inhomogeneously broadened ensemble of oscillators at early times after excitation, which results in a 2D spectrum elongated along the diagonal $\nu_1=\nu_3$. Spectral diffusion destroys this correlation, and the 2D spectrum reshapes

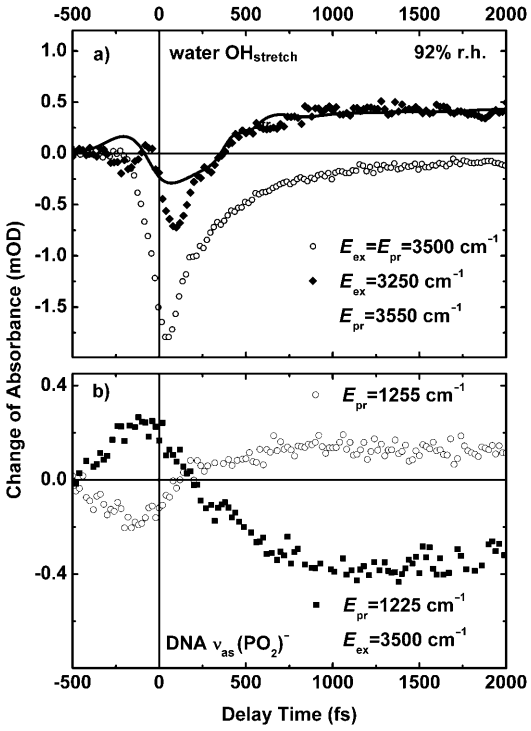

Figure 7. a) Time-resolved change of OH stretching absorption of water in the DNA sample at 92% r.h. (parallel polarization of pump and probe). The data for $E_{ex}=E_{pr}=3500$ cm^{-1} show an initial recovery of ca. 200 fs, followed by a slower 500 fs component and a long-lived residual signal. After excitation at $E_{ex}=3250$ cm^{-1}, an initial decrease in the absorption at $E_{pr}=3550$ cm^{-1} with a recovery of ca. 200 fs is found, followed by an enhancement of absorption, which builds with a time constant of 500 fs. The latter signal is due to the formation of a hot ground state of the water, similar to pure H_2O (solid line, data taken from Ref. [47]). b) Time evolution of the change of $\nu_{as}(PO_2)^-$ absorption of DNA at two fixed probe positions E_{pr} (see Figure 11) after excitation of the OH stretching mode of the surrounding water ($E_{ex}=3500$ cm^{-1}).

towards a round shape. 2D spectra for bulk H_2O (left panel) and for hydrated DNA at 92% r.h. (right panel), recorded after different population (waiting) times T, are presented in Figure 8. The spectra of pure water in the range of the $v=0\rightarrow$ 1 transitions (yellow-red areas) show a transition from an elongated shape at $T=0$ towards a round shape within the first 50 fs. This extremely fast spectral diffusion, which has been discussed in detail in Refs. [40,41], is due to fluctuating forces originating from the fastest librational motions in the hydrogen-bond network. The DNA/water system (right panel) exhibits a pronounced signal component on the diagonal, which is comprised of the NH stretching peaks and the broad OH stretching contribution of water. The cross-peak at a frequency position of $(\nu_3,\nu_1)=(3330$ cm^{-1}, 3200 $cm^{-1})$ results from the coupling between the NH stretching modes at 3200 cm^{-1} and the asymmetric NH_2 stretching mode at 3330 cm^{-1}. The corresponding cross-peak at (3200 cm^{-1}, 3330 cm^{-1}) is masked by the strong signal of opposite sign from the $v=1\rightarrow2$ transitions of the oscillators. At $T=300$ fs, the NH stretching peaks are still at their original positions, that is, their spectral diffusion is minor, while the OH stretching component has strongly reshaped

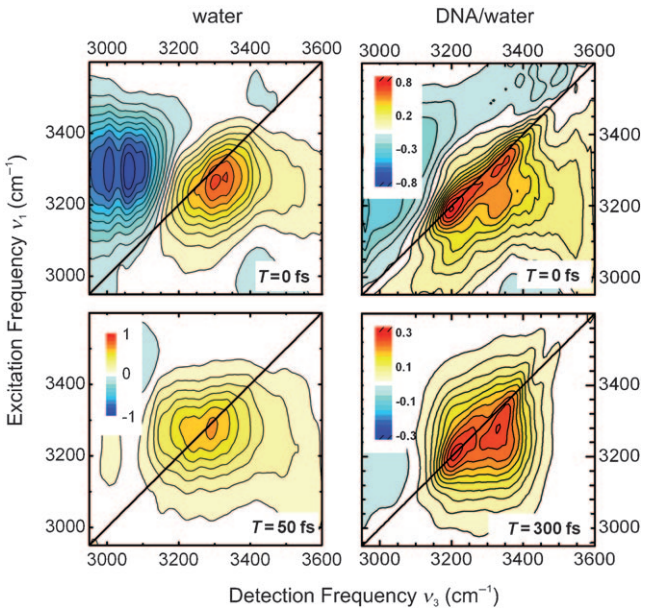

Figure 8. Two-dimensional vibrational spectra of bulk water (left panel, taken from Ref. [40]) and hydrated DNA at 92% r.h. (right panel). The real part of the 2D signal is plotted as a function of excitation frequency ν_1 and the detection frequency ν_3 for different populations (waiting times) T. The signal in the yellow-red areas correspond to the $\nu=0\rightarrow1$ transitions, whereas the blue areas give the $\nu=1\rightarrow2$ signals.

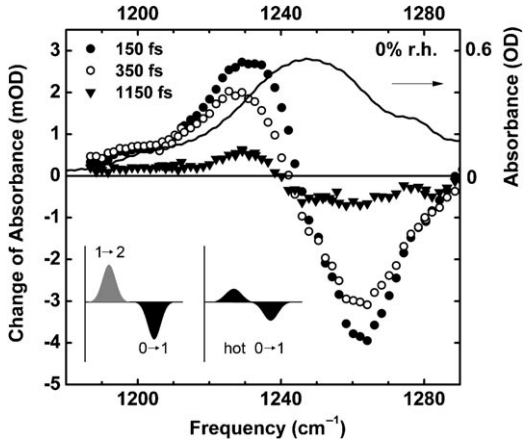

Figure 9. Transient spectra of the asymmetric $\nu_{as}(PO_2)^-$ vibration (symbols) of the DNA oligomers at 0% r.h. after femtosecond excitation by pulses centered at $E_{ex}=1230\ cm^{-1}$. The change of absorbance is plotted as a function of the probe frequency for different pump-probe delays (parallel polarizations of pump and probe). The spectra display the enhanced $\nu=1\rightarrow2$ absorption at low frequencies and the decrease in the $\nu=0\rightarrow1$ absorption at high frequencies (left inset). The right inset shows a schematic representation of the $\nu=0\rightarrow1$ absorption after relaxation of the $\nu=1$ state. Solid line: Linear infrared absorption.

and now displays an essentially round shape. The change in the OH stretching contribution is qualitatively similar to neat H_2O, but occurs on a slower timescale. A more detailed analysis of this behavior and of the vibrational couplings giving rise to the NH off-diagonal peaks will be presented elsewhere.

4.3. Phosphate Vibrations in the DNA Backbone

The ionic phosphate groups in the DNA backbone are important sites of DNA hydration, and their vibrations are sensitive probes of DNA–water interactions. As shown in Figures 1b (inset) and 2c, the asymmetric $(PO_2)^-$ stretching vibration ($\nu_{as}(PO_2)^-$) undergoes a characteristic shift to lower frequencies when the hydration level of DNA increases. In the following, we discuss the first study of the femtosecond dynamics of this mode.

Transient spectra of the $\nu_{as}(PO_2)^-$ absorption at 0% and 92% r.h. were measured after resonant excitation by 130 fs pulses centered at $E_{ex}=1230\ cm^{-1}$. The spectra for 0% r.h. (Figure 9) display an enhanced red-shifted absorption on the $\nu=1\rightarrow2$ transition and a decrease in the absorption of the fundamental ($\nu=0\rightarrow1$) transition. The two components decay with minor changes in their shape and/or spectral position, thus demonstrating negligible spectral diffusion. The red-shift of the enhanced $\nu=1\rightarrow2$ absorption relative to the decrease in the $\nu=0\rightarrow1$ absorption is a measure of the (diagonal) anharmonicity $\Delta\nu$ of the $\nu_{as}(PO_2)^-$ oscillator. A line-shape analysis gives values of $\Delta\nu=\nu_{21}-\nu_{10}=-(12\pm2)\ cm^{-1}$ at 0% r.h. and $\Delta\nu=-(18\pm2)\ cm^{-1}$ at 92% r.h. Both the red-shift and the increase in the anharmonicity of the $\nu(PO_2)^-$ oscillator with relative humidity are due to the increasing hydration level of the phosphate groups. In addition to a larger number of hydrogen bonds between the $(PO_2)^-$ groups and water molecules, the relocation of electronic charge in the highly polarizable $(PO_2)^-$ groups, caused by interaction with the surrounding water dipoles, plays a role here.[75]

At both hydration levels, the enhanced $\nu=1\rightarrow2$ absorption and the decreased $\nu=0\rightarrow1$ absorption show a fast decay with the $\nu=1$ lifetime of 340 fs (Figure 10, solid line: numerical fit). The identical lifetime at 0% and 92% r.h. points to a negligible role of water vibrations in the decay of the $\nu=1$ state. Instead, the coupling to DNA vibrations at lower frequencies, such as the symmetric $(PO_2)^-$ stretching, the diester phosphate stretching, and the phosphate bending modes, is expected to define the pathway for relaxation of the $\nu_{as}(PO_2)^-$ population. After the $\nu=1$ decay, a small longer-lived absorption change is found at 0% r.h. which decays completely within 20 ps. This component, which is also present in the NH stretching kinetics (bottom transient in Figure 10a), reflects the dissipation of excess energy (see Section 5). It is important to note that this slow component is absent for fully hydrated phosphate groups at 92% r.h.

5. Non-Equilibrium Energy Dissipation and Hydration Dynamics

In this section, we address the redistribution of excess energy after vibrational excitation of DNA modes and after excitation of the water shell through the OH stretching band. At 0% r.h., the time-resolved absorption changes of both the $\nu_{as}(PO_2)^-$ and the NH stretching modes at 3190 cm^{-1} (Figure 10a) show—after the decay of the respective $\nu=1$ state—

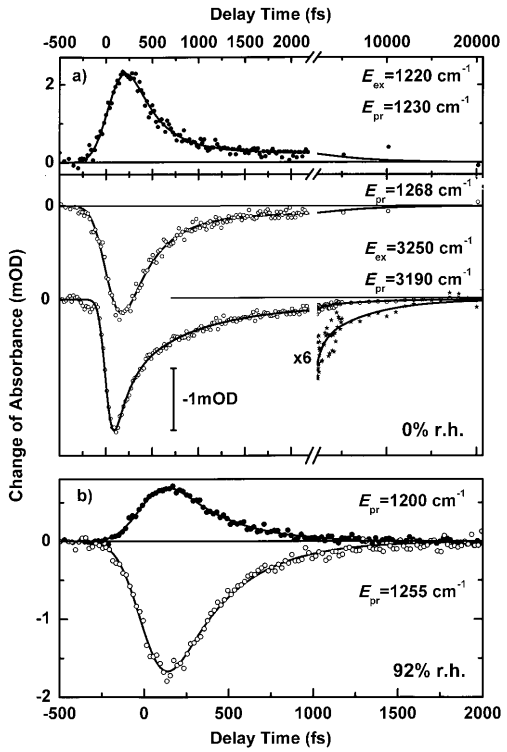

Figure 10. Time-resolved changes of $\nu_{as}(PO_2)^-$ absorption at fixed probe frequencies for DNA oligomers at a) 0% r.h. and b) 92% r.h. (symbols, parallel polarizations of pump and probe). The initial 340 fs decay is independent of the hydration level (solid lines: rate equation fits) and represents the relaxation of the $\nu=1$ population. At 0% r.h., this component is followed by a slow residual signal. This component is also observed in the NH stretching kinetics (bottom transient in (a)) and decays with a time constant of 5.5 ps (solid line). At 92% r.h. (b), the slow signal is absent.

a subsequent longer-lived component that decays within 20 ps. This signal is caused by a reshaping of the respective vibrational band in the hot ground state of the system. More precisely, the excess energy released in the decay of the $\nu=1$ population generates excess populations of low-frequency modes. Some of these modes couple anharmonically to the $\nu_{as}(PO_2)^-$ and/or NH stretching modes, which are now in their $\nu=0$ states. This coupling gives rise to a spectral reshaping of the $\nu_{as}(PO_2)^-$ and/or NH stretching $\nu=0\rightarrow1$ absorption and, thus, to the signal in the picosecond range.[76] Cooling of the low-frequency modes by energy transfer into the large vibrational manifold of DNA is mapped by the slow decay of this "thermal" signal component. At 0% r.h., where only individual water molecules are attached to the phosphate groups providing a correspondingly low density of energy-accepting water vibrations, the main heat sink is DNA itself. Thus, the picosecond decay of the "thermal" signal reflects the time scale of energy transport within and along DNA. It is interesting to note that a very similar time scale has recently been found for the flow of excess vibrational energy along peptide structures[77] and in long-chain hydrocarbons.[78]

For the fully hydrated DNA at 92% r.h., the slow component in the $\nu_{as}(PO_2)^-$ relaxation is absent. Clearly, the water shell around phosphate groups with an excited $\nu_{as}(PO_2)^-$ oscillator serves as a very efficient heat sink. The absence of any slower kinetic component suggests that the energy transfer to the water occurs in a shorter time period than the 340 fs lifetime of the $\nu_{as}(PO_2)^-$ $\nu=1$ state. The energy flow into the water shell is mediated by low-frequency modes. Even if the density of low-frequency vibrational states of a water shell consisting of six water molecules is lower than in bulk water, there is a broad range of librational excitations that can accept the excess energy. Such results establish the important role of the aqueous environment as a sink of excess energy originating from the decay of vibrational and/or vibronic excitations of DNA.

To understand the interaction between the phosphate groups and their water shells in more detail, we performed a series of experiments in which the water shell at 92% r.h. was excited through the OH stretching band and the response of the $\nu_{as}(PO_2)^-$ vibration monitored in a spectrally and temporally resolved way. In Figure 11, transient $\nu_{as}(PO_2)^-$ spectra are plotted for different delay times after excitation at $E_{ex}=3500\ cm^{-1}$. The spectrum taken at -200 fs (probe preceeds pump) reflects the coupling of the OH stretching and the $\nu_{as}(PO_2)^-$ oscillators. At positive time delays (probe after pump), the transient spectra undergo a strong reshaping, and now develop a pronounced decrease in the absorption at low frequencies and an enhanced absorption at high frequencies, both persisting for delay times longer than 10 ps. Time-dependent changes of absorption are shown for fixed probe frequencies in Figure 7b. The transients demonstrate that the modified spectral envelope builds up on the same time scale as the hot ground state of the surrounding water (Figure 7a).

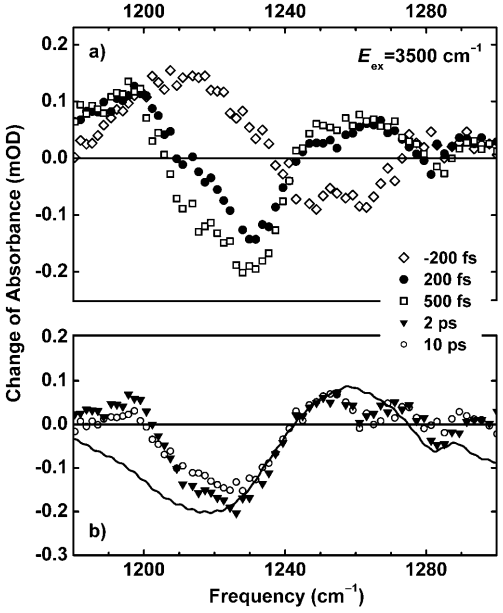

Figure 11. a) Transient spectra (symbols) of the $\nu_{as}(PO_2)^-$ mode after excitation ($E_{ex}=3500\ cm^{-1}$) of the OH stretching mode of water molecules in the DNA sample at high humidity (92% r.h.). Spectra are shown for three different pump-probe delays (parallel polarizations of pump and probe). b) Transient spectra at delay times of 2 and 10 ps (symbols). Solid line: Difference $\delta A=A(0\%)-A(92\%)$ in the linear absorption spectra for 0% and 92% r.h. scaled for the fraction of excited water molecules.

The strong reshaping of the $\nu_{as}(PO_2)^-$ absorption spectrum after OH stretching excitation of the water shell is due to changes in the local water–phosphate interaction, that is, changes in the hydrogen-bond pattern. In the hot ground state of the water shell, there exists a larger fraction of broken hydrogen bonds between water molecules and between water molecules and the $(PO_2)^-$ moieties. As the number of hydrogen bonds decreases, the $\nu_{as}(PO_2)^-$ mode undergoes a transient shift to higher frequencies, which is the behavior found in the transient spectra taken at positive delay times (Figure 11). Under steady-state conditions, a similar shift can be induced by reducing the hydration level of the DNA films (see inset in Figure 1b). The solid line in Figure 11b represents the difference $\delta A = A(0\,\%\,\text{r.h.}) - A(92\,\%\,\text{r.h.})$ of the steady-state $\nu_{as}(PO_2)^-$ spectra for 0% r.h and 92% r.h. This difference spectrum exhibits the same features as the transient spectra—a decrease of absorption at low frequencies and an enhancement at high frequencies. This qualitative agreement between the line shapes in the transient and steady-state difference spectra strongly suggests that a significant fraction of water–phosphate hydrogen bonds are broken in the hot ground state of the water shell.

The smaller number of water–phosphate hydrogen bonds in the hot ground state is equivalent to a reduced water–DNA coupling. In contrast, a strong coupling exists between water molecules in the phosphate hydration shell and water in its surrounding. Thus, the energy flow from the hot water shell into the DNA may be very inefficient, thus favoring the observed very long lifetime of the hot water ground state, which substantially exceeds the 20 ps time interval over which the intra-DNA energy transport occurs.

6. Summary and Outlook

In this Review we have presented very recent work on the ultrafast vibrational dynamics of DNA at different hydration levels. The results demonstrate the potential of nonlinear femtosecond infrared spectroscopy to separate and assign DNA and water vibrations, to determine their couplings, and to unravel microscopic processes governing the dynamics of hydration shells. Polarization-resolved pump-probe studies and 2D vibrational spectra give evidence for the mutual couplings of the different NH stretching modes of adenine–thymine base pairs in the DNA oligomers. In particular, the NH stretching band of thymine and the symmetric NH_2 stretching band of adenine both occur at a frequency of 3200 cm^{-1} and display a coupling strength of the order of 15 cm^{-1}. At a low hydration level (ca. 2 water molecules per base pair), individual water molecules interact with the phosphate groups in the DNA backbone, thereby forming a rigid geometry in which rotation of the water molecules is essentially suppressed. In the case of a fully hydrated DNA, the dynamics of the water shell are closer to those of bulk liquid H_2O with a sub-picosecond spectral diffusion, that is, loss of structural memory, a loss of vibrational anisotropy because of molecular rotations and/or energy transfer, and the formation of a hot ground state of the water after the decay of OH stretching excitations.

The study of the asymmetric $\nu_{as}(PO_2)^-$ stretching vibration gives highly specific insight into the local interaction of water with the ionic phosphate groups in the DNA backbone. The water shell of fully hydrated DNA represents the main heat sink for excess energy released from DNA, with energy transfer in the femtosecond range. In contrast, energy transport within DNA occurs on a slower time scale of about 20 ps. The coupling between the water shell and DNA is reduced in the hot ground state of water, most probably because of a reduced number of water–phosphate hydrogen bonds.

Future work will address vibrational couplings and energy-transfer processes by systematic measurements of two-dimensional infrared spectra, including two-color studies to elucidate couplings between modes of distinctly different frequency. In combination with theoretical calculations, such data will allow for a quantitative analysis of the complex coupling schemes. Another future direction is the study of energy dissipation induced by the radiationless decay of electronically excited states of DNA. In those processes, large amounts of excess energy of the order of 30000 cm^{-1} are redistributed. Femtosecond vibrational spectroscopy is a promising tool to elucidate the pathways of energy flow and, thus, the microscopic mechanisms underlying the high photostability of DNA.

We would like to thank Jason R. Dwyer for his contributions to the results discussed here and Jens Dreyer for his help in generating the cover picture. This work was supported in part by the Deutsche Forschungsgemeinschaft (Sonderforschungsbereich 450) and the Fonds der Chemischen Industrie.

Received: October 9, 2009

[1] J. D. Watson, F. H. C. Crick, *Nature* **1953**, *171*, 737–738.
[2] W. Saenger, *Principles of Nucleic Acid Structure*, Springer, New York, **1984**.
[3] H. Edelhoch, J. C. Osborne, Jr., *Adv. Protein Chem.* **1976**, *30*, 183–250.
[4] H. R. Drew, R. E. Dickerson, *J. Mol. Biol.* **1981**, *151*, 535–556.
[5] W. Saenger, W. N. Hunter, O. Kennard, *Nature* **1986**, *324*, 385–388.
[6] B. Schneider, K. Patel, H. M. Berman, *Biophys. J.* **1998**, *75*, 2422–2434.
[7] M. Tsuboi, *J. Am. Chem. Soc.* **1957**, *79*, 1351–1354.
[8] M. Falk, K. A. Hartman, R. C. Lord, *J. Am. Chem. Soc.* **1962**, *84*, 3843–3846.
[9] M. Falk, K. A. Hartman Jr. , R. C. Lord, *J. Am. Chem. Soc.* **1963**, *85*, 387–391.
[10] B. Prescott, W. Steinmetz, G. J. Thomas, Jr., *Biopolymers* **1984**, *23*, 235–256.
[11] E. Liepinsh, G. Otting, K. Wüthrich, *Nucleic Acids Res.* **1992**, *20*, 6549–6553.
[12] B. Halle, V. P. Denisov, *Biopolymers* **1998**, *48*, 210–233.
[13] A. T. Phan, J. L. Leroy, M. Guéron, *J. Mol. Biol.* **1999**, *286*, 505–519.
[14] A. M. J. J. Bonvin, M. Sunnerhagen, G. Otting, W. F. van Gunsteren, *J. Mol. Biol.* **1998**, *282*, 859–873.
[15] S. Pal, P. K. Maiti, B. Bagchi, *J. Chem. Phys.* **2006**, *125*, 234903.
[16] N. Korolev, A. P. Lyubartsev, A. Laaksonen, L. Nordenskiöld, *Biophys. J.* **2002**, *82*, 2860–2875.
[17] D. Eisenberg, W. Kauzmann, *The structure and properties of water*, Oxford University Press, New York, **1969**.

[18] *Water, a comprehensive treatise* (Ed.: F. Franks), Plenum, New York, **1972**.
[19] I. Ohmine, S. Saito, *Acc. Chem. Res.* **1999**, *32*, 741 – 749.
[20] S. K. Pal, L. Zhao, T. Xia, A. H. Zewail, *Proc. Natl. Acad. Sci. USA* **2003**, *100*, 13746 – 13751.
[21] D. Andreatta, L. Pérez Lustres, S. A. Kovalenko, N. P. Ernsting, C. J. Murphy, R. S. Coleman, M. A. Berg, *J. Am. Chem. Soc.* **2005**, *127*, 7270 – 7271.
[22] S. Sen, D. Andreatta, S. Y. Ponomarev, D. L. Beveridge, M. A. Berg, *J. Am. Chem. Soc.* **2009**, *131*, 1724 – 1735.
[23] S. Pal, P. K. Maiti, B. Bagchi, J. T. Hynes, *J. Phys. Chem. B* **2006**, *110*, 26396 – 26402.
[24] K. E. Furse, S. A. Corcelli, *J. Am. Chem. Soc.* **2008**, *130*, 13103 – 13109.
[25] *Ultrafast infrared and Raman spectroscopy* (Ed.: M. D. Fayer), Dekker, New York, **2001**.
[26] E. T. J. Nibbering, T. Elsaesser, *Chem. Rev.* **2004**, *104*, 1887 – 1914.
[27] R. Laenen, C. Rauscher, A. Laubereau, *Phys. Rev. Lett.* **1998**, *80*, 2622 – 2625.
[28] G. M. Gale, G. Gallot, F. Hache, N. Lascoux, S. Bratos, J. C. Leicknam, *Phys. Rev. Lett.* **1999**, *82*, 1068 – 1071.
[29] S. Woutersen, H. J. Bakker, *Phys. Rev. Lett.* **1999**, *83*, 2077 – 2080.
[30] J. Stenger, D. Madsen, P. Hamm, E. T. J. Nibbering, T. Elsaesser, *Phys. Rev. Lett.* **2001**, *87*, 027401.
[31] J. Stenger, D. Madsen, P. Hamm, E. T. J. Nibbering, T. Elsaesser, *J. Phys. Chem. A* **2002**, *106*, 2341 – 2350.
[32] S. Yeremenko, M. S. Pshenichnikov, D. A. Wiersma, *Chem. Phys. Lett.* **2003**, *369*, 107 – 113.
[33] C. J. Fecko, J. D. Eaves, J. J. Loparo, A. Tokmakoff, P. L. Geissler, *Science* **2003**, *301*, 1698 – 1702.
[34] J. B. Asbury, T. Steinel, K. Kwak, C. P. Lawrence, J. L. Skinner, M. D. Fayer, *J. Chem. Phys.* **2004**, *121*, 12431 – 12446.
[35] R. Rey, K. B. Møller, J. T. Hynes, *J. Phys. Chem. A* **2002**, *106*, 11993 – 11996.
[36] A. Piryatinski, C. P. Lawrence, J. L. Skinner, *J. Chem. Phys.* **2003**, *118*, 9664 – 9671.
[37] A. Piryatinski, C. P. Lawrence, J. L. Skinner, *J. Chem. Phys.* **2003**, *118*, 9672 – 9679.
[38] K. B. Møller, R. Rey, J. T. Hynes, *J. Phys. Chem. A* **2004**, *108*, 1275 – 1289.
[39] J. D. Eaves, A. Tokmakoff, P. L. Geissler, *J. Phys. Chem. A* **2005**, *109*, 9424 – 9436.
[40] M. L. Cowan, B. D. Bruner, N. Huse, J. R. Dwyer, B. Chugh, E. T. J. Nibbering, T. Elsaesser, R. J. D. Miller, *Nature* **2005**, *434*, 199 – 202.
[41] D. Kraemer, M. L. Cowan, A. Paarmann, N. Huse, E. T. J. Nibbering, T. Elsaesser, R. J. D. Miller, *Proc. Natl. Acad. Sci. USA* **2008**, *105*, 437 – 442.
[42] D. Laage, J. T. Hynes, *Science* **2006**, *311*, 832 – 835.
[43] S. Woutersen, H. J. Bakker, *Nature* **1999**, *402*, 507 – 509.
[44] For a recent overview, see *Coherent multidimensional optical spectroscopy* (Eds.: S. Mukamel, Y. Tanimura, P. Hamm), *Acc. Chem. Res.* **2009**, *42*(9), 1207 – 1469.
[45] A. T. Krummel, P. Mukherjee, M. T. Zanni, *J. Phys. Chem. B* **2003**, *107*, 9165 – 9169.
[46] A. T. Krummel, M. T. Zanni, *J. Phys. Chem. B* **2006**, *110*, 13991 – 14000.
[47] A. J. Lock, H. J. Bakker, *J. Chem. Phys.* **2002**, *117*, 1708 – 1713.
[48] N. Huse, S. Ashihara, E. T. J. Nibbering, T. Elsaesser, *Chem. Phys. Lett.* **2005**, *404*, 389 – 393.
[49] S. Ashihara, N. Huse, A. Espagne, E. T. J. Nibbering, T. Elsaesser, *Chem. Phys. Lett.* **2006**, *424*, 66 – 70.
[50] S. Ashihara, N. Huse, A. Espagne, E. T. J. Nibbering, T. Elsaesser, *J. Phys. Chem. A* **2007**, *111*, 743 – 746.
[51] F. Ingrosso, R. Rey, T. Elsaesser, J. T. Hynes, *J. Phys. Chem. A* **2009**, *113*, 6657 – 6665.
[52] R. Rey, F. Ingrosso, T. Elsaesser, J. T. Hynes, *J. Phys. Chem. A* **2009**, *113*, 8949 – 8962.
[53] E. B. Brown, W. L. Peticolas, *Biopolymers* **1975**, *14*, 1259 – 1271.
[54] S. C. Erfurth, E. J. Kiser, W. Peticolas, *Proc. Natl. Acad. Sci. USA* **1972**, *69*, 938 – 941.
[55] Y. Nishimura, K. Morikawa, M. Tsuboi, *Bull. Chem. Soc. Jpn.* **1974**, *47*, 1043 – 1044.
[56] C. Plützer, I. Huenig, K. Kleinermanns, E. Nir, M. S. de Vries, *ChemPhysChem* **2003**, *4*, 838 – 842.
[57] K. Heyne, G. M. Krishnan, O. Kühn, *J. Phys. Chem. B* **2008**, *112*, 7909 – 7915.
[58] G. M. Krishnan, O. Kühn, *Chem. Phys. Lett.* **2007**, *435*, 132 – 135.
[59] J. R. Dwyer, Ł. Szyc, E. T. J. Nibbering, T. Elsaesser, *J. Phys. Chem. B* **2008**, *112*, 11194 – 11197.
[60] P. B. Keller, K. A. Hartman, *Spectrochim. Acta Part A* **1986**, *42*, 299 – 306.
[61] S. Mukamel, *Principles of Nonlinear Optical Spectroscopy*, Oxford, New York, **1995**.
[62] P. Hamm, M. Lim, M. , R. M. Hochstrasser, *J. Phys. Chem. B* **1998**, *102*, 6123 – 6138.
[63] M. C. Asplund, M. T. Zanni, R. M. Hochstrasser, *Proc. Natl. Acad. Sci. USA* **2000**, *97*, 8219 – 8224.
[64] S. Mukamel, *Annu. Rev. Phys. Chem.* **2000**, *51*, 691 – 729.
[65] K. Okumura, A. Tokmakoff, Y. Tanimura, *Chem. Phys. Lett.* **1999**, *314*, 488 – 495.
[66] D. M. Jonas, *Annu. Rev. Phys. Chem.* **2003**, *54*, 425 – 463.
[67] R. A. Kaindl, M. Wurm, K. Reimann, P. Hamm, A. M. Weiner, M. Woerner, *J. Opt. Soc. Am. B* **2000**, *17*, 2086 – 2094.
[68] K. Tanaka, Y. Okahata, *J. Am. Chem. Soc.* **1996**, *118*, 10679 – 10683.
[69] C. Yang, D. Moses, A. J. Heeger, *Adv. Mater.* **2003**, *15*, 1364 – 1367.
[70] C. Y. Yang, W. J. Yang, D. Moses, D. Morse, A. J. Heeger, *Synth. Met.* **2003**, *137*, 1459 – 1460.
[71] Ł. Szyc, J. R. Dwyer, E. T. J. Nibbering, T. Elsaesser, *Chem. Phys.* **2009**, *357*, 36 – 44.
[72] V. Kozich, Ł. Szyc, E. T. J. Nibbering, W. Werncke, T. Elsaesser, *Chem. Phys. Lett.* **2009**, *473*, 171 – 175.
[73] D. Cringus, A. Bakulin, J. Lindner, P. Voehringer, M. S. Pshenichnikov, D. A. Wiersma, *J. Phys. Chem. B* **2007**, *111*, 14193 – 14207.
[74] H. S. Tan, I. R. Piletic, R. E. Riter, N. E. Levinger, M. D. Fayer, *Phys. Rev. Lett.* **2005**, *94*, 057405.
[75] M. Klähn, G. Mathias, C. Kötting, M. Nonella, J. Schlitter, K. Gerwert, P. Tavan, *J. Phys. Chem. A* **2004**, *108*, 6186 – 6194.
[76] P. Hamm, S. M. Ohline, W. Zinth, *J. Chem. Phys.* **1997**, *106*, 519 – 529.
[77] E. H. G. Backus, P. H. Nguyen, V. Botan, R. Pfister, A. Moretto, M. Crisma, C. Toniolo, G. Stock, P. Hamm, *J. Phys. Chem. B* **2008**, *112*, 9091 – 9099.
[78] Z. Wang, J. A. Carter, A. Lagutchev, Y. Kann Koh, N. H. Seong, D. G. Cahill, D. D. Dlott, *Science* **2007**, *317*, 787 – 790.

